



Rational design, synthesis, anti-HIV-1 RT and antimicrobial activity of novel 3-(6-methoxy-3,4-dihydroquinolin-1(2H)-yl)-1-(piperazin-1-yl)propan-1-one derivatives

Subhash Chander^a, Ping Wang^b, Penta Ashok^a, Liu-Meng Yang^b, Yong-Tang Zheng^b, Sankaranarayanan Murugesan^{a,*}

^a Medicinal Chemistry Research Laboratory, Department of Pharmacy, Birla Institute of Technology & Science, Pilani 333031, Rajasthan, India

^b Laboratory of Molecular Immunopharmacology, Key Laboratory of Animal Models and Human Disease Mechanisms of Chinese Academy of Sciences and Yunnan Province, Kunming Institute of Zoology, Chinese Academy of Sciences, Kunming, Yunnan 650223, PR China

ARTICLE INFO

Article history:

Received 20 April 2016

Revised 29 May 2016

Accepted 31 May 2016

Available online 1 June 2016

Keywords:

Tetrahydroquinoline

HIV-1

Reverse transcriptase

AdmetSAR

Docking

Cytotoxicity

ABSTRACT

In the present study, fifteen novel 3-(6-methoxy-3,4-dihydroquinolin-1(2H)-yl)-1-(piperazin-1-yl)propan-1-one (**6a-o**) derivatives were designed as inhibitor of HIV-1 RT using ligand based drug design approach and *in-silico* evaluated for drug-likeness properties. Designed compounds were synthesized, characterized and *in-vitro* evaluated for RT inhibitory activity against wild HIV-1 RT strain. Among the tested compounds, four compounds (**6a**, **6b**, **6j** and **6o**) exhibited significant inhibition of HIV-1 RT ($IC_{50} \leq 10 \mu\text{g/ml}$). All synthesized compounds were also evaluated for anti-HIV-1 activity as well as cytotoxicity on T lymphocytes, in which compounds **6b** and **6l** exhibited significant anti-HIV activity (EC_{50} values 4.72 and 5.45 $\mu\text{g/ml}$ respectively) with good safety index.

Four compounds (**6a**, **6b**, **6j** and **6o**) found significantly active against HIV-1 RT in the *in-vitro* assay were *in-silico* evaluated against two mutant RT strains as well as one wild strain. Further, titled compounds were evaluated for *in-vitro* antibacterial (*Escherichia coli*, *Pseudomonas putida*, *Staphylococcus aureus* and *Bacillus cereus*) and antifungal (*Candida albicans* and *Aspergillus niger*) activities.

© 2016 Elsevier Inc. All rights reserved.

1. Introduction

Acquired Immune Deficiency Syndrome (AIDS) pandemic continues to be a major public health issue worldwide [1,2]. According to a report published in 2014 on statistics of AIDS, around 36.9 million people (including 2.6 million children) were living with HIV globally with prevalence of 0.8% [3], in the same year, around 1.2 million people died due to AIDS and related diseases [4]. Non-nucleoside reverse transcriptase inhibitors (NNRTIs) are structurally diverse group of compounds which binds to allosteric site of HIV-1 RT and inhibits its catalytic function [5–7]. NNRTIs are important part of Highly Active Antiretroviral Therapy (HAART) due to their less toxicity, high specificity and unique antiviral potency. But like other anti-HIV drugs, effectiveness of currently approved NNRTIs has been hampered due to the rapid development of drug resistance [8,9]. For example, two mutant strains of

HIV-1 RT; K103N and K103N/Y181C are frequently observed clinically in patients on NNRTIs therapy [10]. Single mutation K103N in HIV-1 RT generally reduces its sensitivity towards the first line drugs (specially efavirenz), while dual mutation (K103N/Y181C) generally confer resistance against the first as well second line drugs except rilpivirine [11]. To circumvent this problem, there is an urgent need to discover novel NNRTIs having good potency against wild as well as mutant RT strains, less toxicity and improved physicochemical properties.

1,2,3,4-Tetrahydroquinoline (THQ) nucleus containing organic compounds have privileged position in the medicinal chemistry, such compounds are reported for diverse biological activities like antiviral, antimicrobial, antifungal, antileishmanial, antimalarial, antitubercular, antidiabetic, antithrombotic and anticancer [8,12–17]. Exploring the anti-HIV-1 activity of compounds containing tetrahydroquinoline nucleus, Su and team reported a series of compounds which exhibited potent inhibitory activity against HIV-1 RT by blocking its allosteric site. Most potent compound of the series **A1** (Fig. 1) exhibited inhibitory activity against wild, as well as double mutant strain (K103N and Y181C) of HIV-1 RT with

* Corresponding author.

E-mail addresses: zhengyt@mail.kiz.ac.cn (Y.-T. Zheng), murugesan@pilani.bits-pilani.ac.in (S. Murugesan).

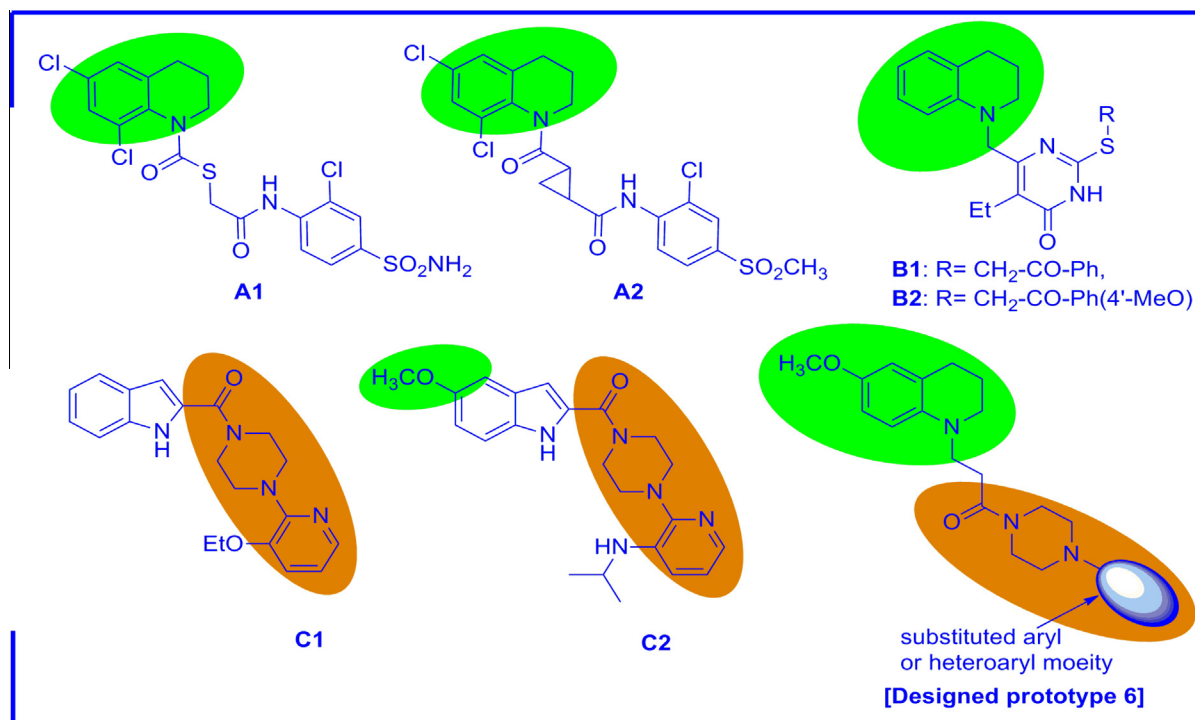


Fig. 1. Literature reported potent HIV-1 RT inhibitors and the designed prototype compound.

IC₅₀ values of 1.1 and 4 nM respectively. Another bioisostere of the same compound **A2** (Fig. 1) also inhibited the activity of both selected RT strains with IC₅₀ values of 18 and 99 nM respectively [18]. In another study, a novel series of 5-alkyl-2-arylthio-6-((3,4-dihydroquinolin-1(2H)-yl)methyl)pyrimidin-4(3H)-ones were synthesized and evaluated for HIV-1 RT inhibitory activity, in which compounds **B1** and **B2** (Fig. 1) exhibited potency comparable to nevirapine [19]. Further, several studies have revealed that, compounds like **C1** and **C2** (Fig. 1) containing 1-(4-(pyridin-2-yl)piperazin-1-yl)ethanone moiety attached with indole nucleus inhibited the activity of HIV-1 RT at low micromolar concentration. Molecular hybridization by combination of two or more pharmacophoric subunits of known bioactive moieties is an emerging and rational approach to design novel ligands against a specific target [20]. In the present study, using the structural features of known RT inhibitors, we designed scaffold **6** as inhibitor of HIV-1 RT (Fig. 1). Further, series of compounds (**6a-o**) were generated by making different substitution at the aryl or heteroaryl group of scaffold **6**.

ADMET (Absorption, Distribution, Metabolism, Excretion and Toxicological) properties play indispensable role in early stages of drug discovery and development. Therapeutic drugs possess a balance of suitable ADMET properties and intrinsic potency. However, determination of ADMET of all novel molecules using *in-vivo* models is very challenging, costly and time consuming task. So, in order to predict the drug-likeness behavior of the designed compounds, we *in-silico* generated these properties using three different tools; Qik-prop module of Schrödinger [21], admetSAR [22] and FAF-Drugs [23].

People living with HIV/AIDS face major health threats due to their weak immune system, which make them susceptible to infections called "opportunistic infections" (OIs), which are the most common cause of death among HIV/AIDS patients [24,25]. Among the various "opportunistic infections" associated with HIV/AIDS, various bacterial and fungal borne infections contribute a major role. Moreover, emerging drug resistance of bacterial and fungal pathogen towards

the currently available therapy further drive the need for the search of new potential antibacterial and antifungal agents. Many studies revealed the antibacterial [26–28] and antifungal potential of compounds containing THQ nucleus [29–31]. Moreover, phenylpiperazine moiety present in the designed compounds is also present in marketed antifungal drugs like ketoconazole and itraconazole. So all these facts provoked us for the evaluation of synthesized compounds against the bacterial (*Escherichia coli*, *Pseudomonas putida*, *Staphylococcus aureus* and *Bacillus cereus*) and fungal strains (*Candida albicans* and *Aspergillus niger*).

2. Results and discussion

2.1. In-silico prediction of physicochemical and ADMET parameters

Physicochemical and ADMET parameters of the synthesized compounds were *in-silico* predicted (Table 1) using Qikprop module of Schrödinger as well as online tools admetSAR and FAF-Drug. The predicted values of parameters like Mol Wt, HBD, HBA, ClogP were found within their acceptable range and followed the Lipinski rule of five. Parameters like SASA (represents total solvent accessible surface area in square angstroms), logS (represent aqueous solubility, in mol dm⁻³), PCaco (represent apparent Caco-2 cell permeability in nm/s, which correlates with permeability of compound across the membrane of gut cell), logBB (represent brain/blood partition coefficient) were also found within their optimum range. According to the predicted acute oral toxicity values, all the compounds lie in "class III", compounds of this class possessed fairly high lethal dose and generally considered suitable for the druggable point of view. Further, mutagenicity of all compounds was predicted in qualitative terms, in this study, none of the compounds possessed mutagenicity. So, overall predicted physicochemical and ADMET parameters of compounds **6a-o** were found within the optimum range (Table 1, supplementary data) of drug likeness [32].

Table 1
In-silico predicted drug likeness parameters of the titled compounds.

Comp. code	Mol Wt	SASA ^a	HBD ^b	HBA ^c	ClogP	logS	PCaco ^d	logBB ^e	Rot ^f	Acute tox. ^g
6a	379.23	690.49	0	5	4.14	−4.77	2585.16	−0.07	4	Class III
6b	393.24	723.60	0	5	4.40	−5.53	2579.47	−0.09	4	Class III
6c	393.24	733.17	0	5	4.41	−5.68	2397.01	−0.13	4	Class III
6d	409.24	744.73	0	6	4.35	−5.25	2576.60	−0.16	5	Class III
6e	409.24	733.78	0	6	4.22	−5.04	2404.41	−0.18	5	Class III
6f	409.24	738.23	0	6	4.22	−5.12	2397.01	−0.19	5	Class III
6g	397.22	705.34	0	5	4.34	−5.20	2467.31	−0.02	4	Class III
6h	397.22	710.01	0	5	4.40	−5.35	2398.53	0.00	4	Class III
6i	413.19	722.55	0	5	4.66	−5.62	2585.25	0.05	4	Class III
6j	413.19	724.89	0	5	4.67	−5.73	2397.39	0.05	4	Class III
6k	413.19	725.02	0	5	4.67	−5.74	2398.21	0.05	4	Class III
6l	424.21	739.36	0	8	3.41	−5.01	287.89	−1.21	5	Class III
6m	393.24	738.53	0	5	3.62	−3.61	643.76	0.18	6	Class III
6n	380.22	696.67	0	6	3.81	−4.64	2186.13	−0.16	4	Class III
6o	447.15	742.58	0	5	4.97	−6.25	2585.43	0.18	4	Class III

^a Solvent accessible surface area.

^b No. of hydrogen bond donors.

^c No. of hydrogen bond acceptors.

^d Predicted apparent Caco-2 cell permeability.

^e Predicted brain/blood partition coefficient.

^f No. of rotatable bonds.

^g Acute toxicity.

2.2. Chemistry

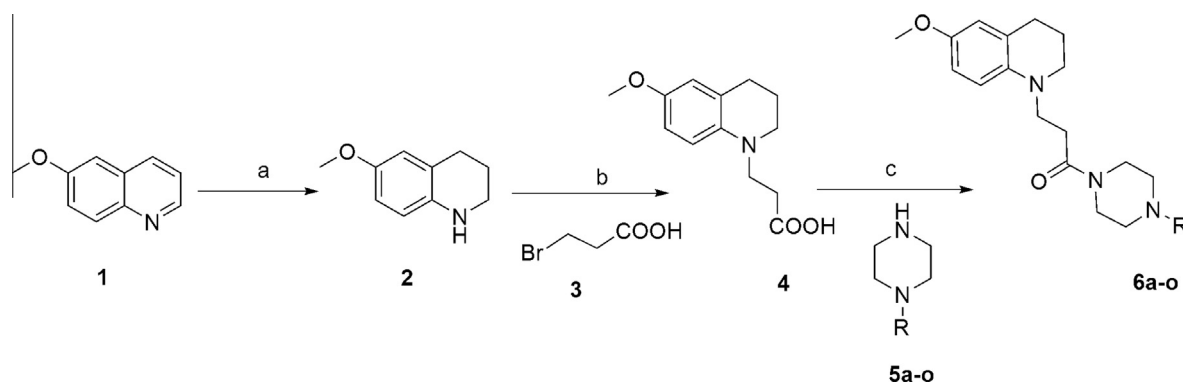
Designed compounds **6a–o** were synthesized using three step synthetic route, reaction conditions used for the synthesis of target compounds are shown in [Scheme 1](#). First step involved the reduction of 6-methoxyquinoline (**1**) into 6-methoxytetrahydroquinoline **2** using Nickel-aluminium alloy under basic condition. Further, coupling of intermediate **2** with 3-bromopropanoic acid **3**, afforded intermediate **4**. Finally, coupling of intermediate **4** with substituted piperazine (**5a–o**) afforded titled compounds **6a–o**.

Purified compounds were characterized preliminarily by non-spectral methods like melting point and thin layer chromatography and final structures were confirmed by spectral analysis like IR, ¹H NMR and Mass spectroscopy. The IR spectra of compounds (**6a–o**) showed the expected absorption bands, for example corresponding to stretching of amide carbonyl adjacent to the piperazine (C=O) peak appeared at 1635–1690 cm^{−1}. Absorption band of (C–O–C) stretching corresponding to the 6-methoxy group of THQ appeared at around 1242–1230 cm^{−1}. ¹H NMR spectrum of the reported compounds exhibited characteristic multiplet around δ 1.97–1.95 corresponding to the two protons at the 3rd position of THQ ring, while two protons at the fourth position displayed peaks (dd or multiplet) near δ 2.64–2.65. Protons at the carbon adjacent to the keto group appeared as triplet (also multiplet in some compounds) near δ 2.74–2.76, while three protons of 6-methoxy group

appeared as singlet at δ 3.75. Other ¹H NMR signals and proton counting of all the titled compounds were also observed in their expected region. ESI-MS of the synthesized compounds showed the corresponding M+1 peak. Elemental analysis (C, H and N) indicated that, the calculated and observed values were within the acceptable limits. Spectral characterization data of synthesized compounds **6a–o** are given in the supplementary part of the manuscript.

2.3. HIV-1 RT inhibitory activity

Purified and characterized compounds were screened for the HIV-1 RT inhibitory activity using RT assay kit (Roche) and marketed drug efavirenz was used as reference compound. The results of RT *in-vitro* assay revealed that, out of fifteen tested compounds, four (**6a**, **6b**, **6j** and **6o**) exhibited significant (IC₅₀ ≤ 10 μg/ml, highlighted in bold font in [Table 2](#)), seven (**6c**, **6d**, **6e**, **6g**, **6i**, **6k** and **6n**) exhibited moderate (IC₅₀ > 10 to ≤ 30 μg/ml), while rest of compounds exhibited weak activity (IC₅₀ > 30 μg/ml). Compound with un-substituted phenyl ring (**6a**) exhibited significant inhibitory potential against RT (IC₅₀ 9.20 μg/ml). Further, substitution of phenyl with methyl group at *ortho* position increased the potency against RT (IC₅₀ 4.91 μg/ml), while at *para* position, it decreased the potency (IC₅₀ 28.46 μg/ml). Further, substitution with more electron releasing groups like methoxy decreased the



Scheme 1. Reagents and conditions: (a) EtOH, 10% aq. NaOH, Ni–Al alloy, 0 °C–rt 6 h (b) ACN, Et₃N, reflux 5 h (c) HOBT, EDC·HCl, Et₃N, DCM, rt, 6–8 h.

Table 2
Result of *in-vitro* HIV-1 RT inhibition activity of the titled compounds.

Comp. code	R	HIV-1 RT activity (IC ₅₀ in μM) ^a	HIV-1 RT activity (IC ₅₀ in μg/ml)	anti-HIV-1 activity (μg/ml)	Cytotoxicity (μg/ml)	Safety index
6a	Ph	24.26	9.20	14.21	83.21	5.9
6b	2-Me-Ph	12.48	4.91	4.72	114.33	24.2
6c	4-Me-Ph	28.46	11.19	14.98	86.18	5.8
6d	2-MeO-Ph	52.84	21.62	13.21	80.80	6.1
6e	3-MeO-Ph	58.24	23.83	20.43	110.08	5.4
6f	4-MeO-Ph	>100	>40.92	21.54	95.67	4.4
6g	2-F-Ph	47.45	18.85	17.89	82.89	4.6
6h	4-F-Ph	78.48	31.17	19.43	85.82	4.4
6i	2-Cl-Ph	32.86	13.58	11.04	112.23	10.2
6j	3-Cl-Ph	18.58	7.68	18.38	97.51	5.3
6k	4-Cl-Ph	24.91	10.29	16.43	95.82	5.7
6l	4-NO ₂ -Ph	82.68	35.07	5.45	>200	>36.7
6m	Benzyl	>100	>39.32	43.79	94.51	2.2
6n	2-Pyridine	48.62	18.49	21.07	98.84	4.7
6o	2,3-DiCl-Ph	14.46	6.47	17.40	104.10	6
Efavirenz		0.025	0.0078			
Zidovudine				0.0034	1565.72	460505.88

^a Value is mean of duplicate experiment, each value exhibited SD less than ±10% from mean.

potency against RT at all positions. Among these *ortho* and *meta* substituted compounds, **6d** and **6e** did not showed significant difference in their potency, however, substitution at *para* position of phenyl ring (**6f**) significantly decreased the potency. Fluoro substituted compounds at *ortho* and *meta* position (**6g** and **6h**) exhibited moderate to weak inhibition of HIV-1 RT (IC₅₀ 18.85 and 31.17 μg/ml respectively). Three chloro substituted compounds (**6i**, **6j** and **6k**) showed relatively good potency against RT, in which *meta* substituted compound **6j** significantly inhibited the activity of RT with IC₅₀ 7.68 μg/ml, while *para* nitro substituted compound **6l** exhibited weak inhibition of RT. Compound in which phenyl ring was replaced with benzyl (**6m**) and 2-pyridine (**6n**) exhibited weak and moderate inhibition of HIV-1 RT (>39.32 and 18.49 μg/ml respectively). Compounds having di-substitution with chloro at *ortho* and *meta* position of phenyl ring also exhibited significant inhibition of HIV-1 RT (IC₅₀ 6.47 μg/ml). Standard drug efavirenz showed promising activity against HIV-1 RT with IC₅₀ 0.0078 μg/ml.

2.4. Cytotoxicity and anti-HIV activity

The result of anti-HIV-1 activity and cytotoxicity studies of compounds **6a-o** are shown in Table 2. Compounds **6b** and **6l** exhibited significant activity (EC₅₀ values of 4.72 and 5.45 μg/ml respectively) against HIV mediated syncytia formation with overall good safety index 24.2 and >36.7 respectively. Interestingly, compound **6b** not only showed significantly activity against HIV-1 RT, but also retained the significant potency against HIV-1. Further, compound **6l** showed weak RT inhibitory activity, but it showed significant anti-HIV-1 activity, so it may have different mechanism of action. Reference drug zidovudine showed promising anti-HIV-1 activity (EC₅₀ 0.0034 μg/ml), with least cytotoxicity (CC₅₀ 1565.72 μg/ml).

2.5. Docking studies

Four compounds (**6a**, **6b**, **6j** and **6o**) which exhibited significant *in-vitro* RT inhibitory activity were further *in-silico* evaluated against two mutant strains as well as one wild strain (for comparison) of HIV-1 RT. Wild strain of HIV-1 RT exhibited no mutation (Pdb ID: 4G1Q), among the mutant strains first involved; K103N (Pdb ID: 3TAM), and other mutant strain exhibited dual mutation K103N/Y181C (Pdb ID: 4I2Q) at the NNIBP (Non Nucleoside Inhibitory Binding Pocket).

The value of RMSD obtained between experimental binding mode as in X-ray and re-docked poses of co-crystallized ligands of three proteins (3MEE, 3TAM and 4I2Q) were found to be 0.6, 1.1 and 0.9 respectively. So, validation study revealed that, docking procedure could be relied on for further docking studies, superimpose view of rilpivirine X-ray pose and its redock pose in 3MEE is shown in Fig. 2 as one of representative. Docking results of ligands **6a**, **6b**, **6j** and **6o** along with the reference rilpivirine against three selected proteins is shown in Table 3.

Result of docking studies (Table 3) revealed that, among the four compounds, two exhibited moderate (**6a** and **6o**) and two (**6b** and **6j**) exhibited good *in-silico* potency against the wild 3MEE strain based upon the Glide score (G score). Further, compounds **6a** and **6b** exhibited moderate while **6j** and **6o** exhibited weak potency against the single mutant 3TAM strain. While against the dual mutant strain (4I2Q), compound **6j** exhibited weak while three compounds (**6a**, **6b** and **6o**) exhibited moderate potency. Further, putative binding modes of compound **6b** within NNIBP of three RT strains were analyzed (Figs. 3 and 4). The best docked pose of compound **6b** exhibited prominent hydrophobic interaction with residues like Tyr-181 (with Cys-181 in 4I2Q), Tyr-188, Phe-227, Trp-229, Leu-234, and Tyr-318 in all three selected strains. Further, **6b** also exhibited hydrophobic interaction with other residues of different RT strains like Val-179 of 3MEE, Pro-95, Leu-100, Pro-225, Pro-236 of 3TAM and Val-179, Val-100, Tyr-183 of 4I2Q. It was noteworthy that, keto group adjacent to the piperazine ring of **6b** exhibited dual hydrogen bonding interaction with the hydrophilic residues Lys-101 and Lys-103 of 3MEE (Fig. 3) which further enhance its binding affinity with 3MEE, but unfortunately similar interaction were not observed in 3TAM and 4I2Q (Fig. 4). The absence of hydrogen bonding interaction in 3TAM and 4I2Q may be due to the mutations (K103N and Y181C) that resulted in disorientation inside the NNIBP pocket. Consequently, keto group of ligand **6b** was also not able to interact with Lys-101. So, overall docking study revealed that, compounds **6a**, **6b**, **6j** and **6o** displayed good to moderate affinity against the wild RT strain (3MEE) when compared to reference drug rilpivirine, while against the two mutant strains (3TAM and 4I2Q) these exhibited moderate to weak affinity.

2.6. Antimicrobial activity

Antimicrobial activity of the synthesized compounds against four selected bacterial strains and two fungal strains are shown

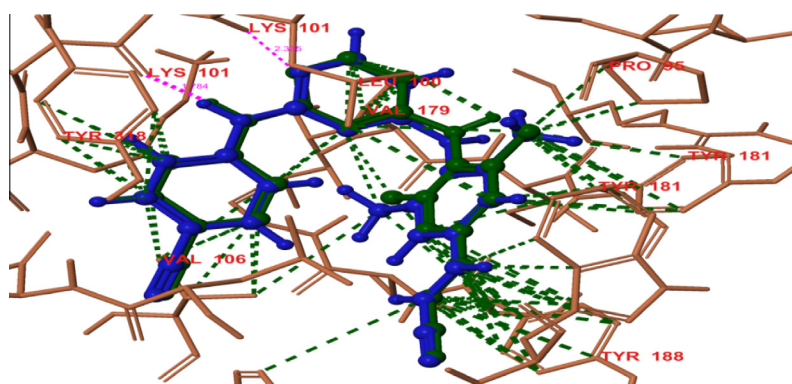


Fig. 2. Superimposed view of best scoring pose of rilpivirine (blue) with its X-ray pose (green) in 3MEE.

Table 3
Glide score of significantly active compounds and rilpivirine against three RT strains.

Comp. code	G score (3MEE)	G score (3TAM)	G score 4IQ2
6a	-12.22	-9.46	-9.24
6b	-13.37	-9.34	-9.17
6j	-13.18	-8.17	-7.92
6o	-12.07	-8.72	-9.38
Rilpivirine	-14.32	-11.83	-11.36

in **Tables 4 and 5** respectively. Based upon the values of ZOI in mm, compounds are classified; as significantly active (ZOI ≥ 15 , highlighted in bold font in **Tables 4 and 5**), moderately active (ZOI 13–14), weakly active (ZOI 10–12) and least active (ZOI less than 10). MIC was not calculated for compounds which showed ZOI less than 10 mm.

2.6.1. Antibacterial activity

Among the series of compounds **6a–o**, twelve compounds showed moderate to significant inhibitory activity against *E. coli*. Among these, eight compounds (**6a**, **6c**, **6e**, **6g**, **6i**, **6j**, **6k** and **6o**) showed moderate while remaining four compounds (**6d**, **6f**, **6l** and **6n**) showed significant inhibitory potential (**Table 4**). Also, eight compounds exhibited inhibitory potential against the growth of *S. aureus*, in which two compounds (**6k** and **6n**) showed significant, five compounds (**6a**, **6b**, **6e**, **6f** and **6i**) exhibited moderate

and one compound (**6g**) showed weak inhibition. Further, one compound **6n** showed significant, seven compounds (**6b**, **6e**, **6d**, **6f**, **6h**, **6i** and **6l**) showed moderate, while rest of the compounds exhibited weak to least inhibition against *P. putida*. Similarly, five compounds (**6a**, **6d**, **6f**, **6l** and **6n**) showed significant, six compounds (**6b**, **6c**, **6e**, **6i**, **6j** and **6m**) showed moderate while rest of the compounds showed weak to least activity against *B. cereus*. Interestingly, three compounds (**6d**, **6f** and **6l**) exhibited significant growth inhibition of G(–)ve bacteria *E. coli* as well as G(+ve) *B. cereus*, while compound **6n** significantly inhibited the growth of all tested bacterial strains.

2.6.2. Antifungal activity

Among the tested compounds (**6a–o**), seven compound (**6a**, **6c**, **6e**, **6f**, **6h**, **6l** and **6n**) showed significant, one compound **6i** exhibited moderate, while rest of the compounds possessed weak to least antifungal activity against *C. albicans* (**Table 5**). Against the second fungal strain (*A. niger*), seven compounds (**6b**, **6d**, **6f**, **6j**, **6k**, **6l** and **6n**) exhibited significant, five compounds (**6a**, **6c**, **6e**, **6h** and **6m**) showed moderate, while rest of the compounds displayed weak to least inhibitory potential. Interestingly, three compounds (**6f**, **6l** and **6n**) significantly inhibited the growth of both the tested fungal strains. Moreover, compound **6n** showed promising antifungal activity against *C. albicans* and *A. niger* with ZOI 19, 20 mm and MIC 32, 16 $\mu\text{g/ml}$ respectively.

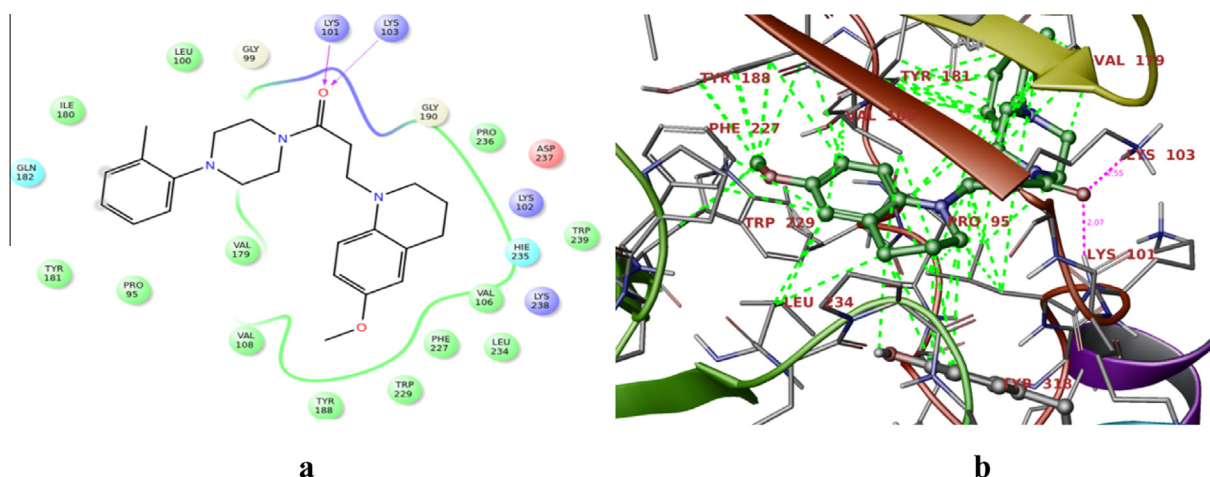


Fig. 3. Docked pose of **6b** inside the NNIBP of 3MEE showing two-dimensional interactive diagram (**3a**), showing hydrophobic and hydrogen bond interaction represented by green and pink dotted lines respectively (**3b**).

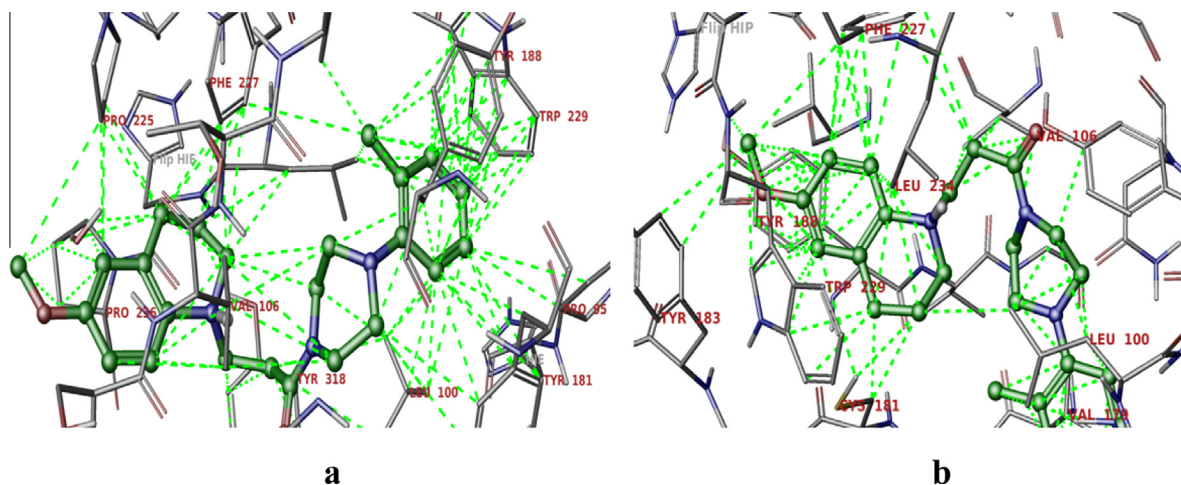


Fig. 4. Docked pose of **6b** inside the NNIBP of 3TAM (**4a**) and 4I2Q (**4b**) showing hydrophobic interaction represented by green dotted lines.

Table 4
Result of antibacterial activity of the titled compounds.

Comp. code	<i>E. coli</i>		<i>S. aureus</i>		<i>P. putida</i>		<i>B. cereus</i>	
	Zone of inhibition (mm)	MIC ($\mu\text{g/ml}$)	Zone of inhibition (mm)	MIC ($\mu\text{g/ml}$)	Zone of inhibition (mm)	MIC ($\mu\text{g/ml}$)	Zone of inhibition (mm)	MIC ($\mu\text{g/ml}$)
6a	14	>128	13	>128	12	>128	15	>64
6b	–	–	14	>64	14	>128	14	>64
6c	13	>64	–	–	12	>128	13	>128
6d	15	>64	–	–	13	>128	15	64
6e	14	>128	14	>128	14	>64	13	>128
6f	17	>32	14	>128	14	>64	16	64
6g	13	>128	12	>128	–	–	–	–
6h	–	–	–	–	13	>128	12	>128
6i	14	>128	13	>128	13	>128	13	>128
6j	14	>128	–	–	–	–	14	>64
6k	13	>128	15	>64	11	>128	–	–
6l	15	>64	–	–	14	>128	15	>64
6m	–	–	–	–	12	>128	13	>128
6n	18	32	15	>128	16	64	15	>128
6o	13	>128	–	–	12	>128	11	>128
Chloramphenicol	22	16	22	16	23	16	21	16

Table 5
Result of antifungal activity of the titled compounds.

Compound	<i>Candida albicans</i>		<i>Aspergillus niger</i>	
	ZOI (mm)	MIC ($\mu\text{g/ml}$)	ZOI (mm)	MIC ($\mu\text{g/ml}$)
6a	16	64	13	128
6b	12	>128	15	64
6c	15	128	14	>64
6d	–	–	18	32
6e	16	64	14	>64
6f	19	>32	17	32
6g	–	–	11	>128
6h	16	64	14	64
6i	14	128	–	–
6j	–	–	15	64
6k	12	>128	16	>64
6l	18	>32	17	32
6m	–	–	14	>64
6n	19	32	20	16
6o	11	>128	–	–
Fluconazole	21	8	22	8

3. Experimental

3.1. In-silico prediction of physicochemical and ADMET parameters

Physicochemical and ADMET parameters of the designed compounds were *in-silico* predicted using the Qikprop module of Schrödinger, admetSAR and FAF-Drugs³. Different drug likeness parameters were predicted like; molecular weight, number of hydrogen bond donor, number of hydrogen bond acceptor, total solvent accessible surface area, octanol/water partition coefficient, aqueous solubility, apparent caco-2 cell permeability, brain/blood partition coefficient, number of violations of Lipinski's rule of five, number of rotatable bonds, rat acute toxicity and mutagenicity.

3.2. Chemistry

All solvents and reagents purchased from Sigma or SD fine companies were used as received without further purification.

The progress of reaction was monitored by thin layer chromatography (TLC) using ethyl acetate and hexane (in suitable proportion) as mobile phase. Melting points were uncorrected and determined in open capillary tubes on a Precision Buchi B530 (Flawil, Switzerland) melting point apparatus containing silicon oil. The IR spectra of the synthesized compounds were recorded using FTIR spectrophotometer (Shimadzu IR Prestige 21, Shimadzu, Mumbai, India). ¹H NMR spectra were recorded on Bruker DPX-400 spectrometer (Bruker India Scientific Pvt. Ltd., Mumbai, India) using TMS as an internal standard (chemical shifts in δ). Elemental analysis was performed on Vario EL III M/s Elementar C, H, N, and S analyzer (Elementar Analysensysteme GmbH, Hanau, Germany). ESI-MS were recorded on MICROMASS Quattro-II LCMS system (Waters Corporation, Milford, USA).

3.2.1. Synthesis of 6-methoxy-1,2,3,4-tetrahydroquinoline (2)

To the stirred solution of 6-methoxyquinoline **1** (5 g, 31.44 mmol) in ethanol, Ni-Al alloy (2.5 g) was added and stirring was continued for 30 min. Further, reaction mass was cooled to 0–4 °C and then aqueous sodium hydroxide solution (10% w/v, 50 ml) was added slowly. After the complete addition, reaction mixture was further stirred at room temperature for 6 h. After completion of reaction as per TLC, reaction mass was passed through a tight celite bed, further ethanol (2 × 75 ml) was passed through the celite bed. Combined filtrate was evaporated on rotary evaporator till its volume remained one-fourth to its original volume. Further, reaction mass was acidified with 2 N HCl, until its pH became neutral. Further, reaction mass was taken in separating funnel and extracted twice with ethyl acetate (2 × 150 ml). Combined ethyl acetate layer was first washed with water (300 ml) and then with brine (300 ml). Ethyl acetate layer was dried over anhydrous sodium sulphate and finally evaporated on rotary evaporator to afford the compound **2** as crude oil. Crude **2** was purified by column chromatography using 5% ethyl acetate in hexane as mobile phase and silica (mesh size 100–200) as stationary phase, which afforded the pure compound **2**, as light yellow oil with 87% yield [33].

3.2.2. Synthesis of 3-(6-methoxy-3,4-dihydroquinolin-1(2H)-yl)propanoic acid (4)

3-Bromopropanoic acid **3** (2.67 g, 21.4 mmol) was added portion wise to the stirring solution of 6-methoxy-1,2,3,4-tetrahydroquinoline **2** (3.5 g, 21.4 mmol) in acetonitrile, containing triethyl amine (5.40 g, 53.5 mmol) as base and catalytic amount of potassium iodide. Reaction mixture was refluxed and progress of the reaction was monitored using TLC. After completion of reaction, as per TLC (after 5 h), acetonitrile was evaporated on rotary evaporator, 100 ml of water was added to reaction mixture and extracted with hexane (150 ml). Further, aqueous layer was separated and neutralized with 6 N HCl, and taken in a separating funnel, and twice extracted with ethyl acetate (2 × 250 ml). Combined ethyl acetate layer was first washed with water (250 ml) and then subsequently with brine (250 ml). Ethyl acetate layer was dried over anhydrous sodium sulphate and finally evaporated on rotary evaporator to afford compound **4** as light yellow semisolid with 73% yield.

3.2.3. General procedure for the synthesis of 3-(6-methoxy-3,4-dihydroquinolin-1(2H)-yl)-1-(4-phenylpiperazin-1-yl)propan-1-one derivatives (6a-o)

To the stirred solution of 3-(6-methoxy-3,4-dihydroquinolin-1(2H)-yl) propanoic acid **4** (0.235 g, 1 mmol) in dry DCM, HOBt (0.16 g, 1.2 mmol) and EDCI·HCl (0.23 g, 1.2 mmol), triethyl amine (0.253 g, 2.5 mmol) were added and stirring was continued for 30 min. at room temperature. To the reaction mixture, corresponding piperazines (**5a-o**) were added and the reaction mixture was

further stirred at room temperature for 6–8 h. After completion of reaction as per TLC, reaction mass was taken in a separating funnel, to this 25 ml more DCM was added, and organic layer was washed with saturated sodium bicarbonate solution (50 ml). Organic layer was then washed with distilled water (50 ml), DCM layer was separated and dried over anhydrous sodium sulphate and finally evaporated to afford the final compounds **6a-o** [34].

3.3. In-vitro HIV-1 RT screening

In-vitro HIV-1 RT inhibitory activity of the synthesized compounds was evaluated using Roche diagnostics kit in accordance with the kit protocol [35]. This is based upon colorimetric assay method in which marketed drug efavirenz was used as reference compound. Procedure followed is briefly described here; the reaction mixture was set with template primer complex, RT enzyme and dNTPs in a lysis buffer with or without inhibitors. The reaction mixture was incubated at 37 °C for 1 h and then transferred to streptavidin-coated microtitre plate (MTP). The biotin-labeled dNTPs that were incorporated in the template due to activity of RT, bound to streptavidin. The unbound dNTPs were washed using wash buffer and anti-DIG-POD was added to the MTP. The DIG-labeled dNTPs incorporated in the template were bound to an anti-DIG-POD antibody. The unbound anti-DIG-POD was washed again with washing buffer and the peroxide substrate (ABST) was added to the MTP. A colored reaction product was produced during the cleavage of the substrate catalyzed by a peroxide enzyme. The absorbance of the sample was determined as an optical density (OD) at 405 nm using a micro titer plate ELISA reader. The final value of OD taken is average of duplicate results and % inhibition of HIV-1 RT was calculated using the below mentioned formula. Initially, compounds were screened at 100 μ M concentration, finally IC₅₀ was calculated using double dilution method.

$$\% \text{ Inhibition} = 100 - \left(\frac{\text{OD at 405 nm with inhibitor}}{\text{OD at 405 nm without inhibitor}} \right) \times 100$$

3.4. Cytotoxicity and anti-HIV activity

Synthesized compounds **6a-o** were evaluated for cytotoxicity upon the CD4⁺ line of T cells (C8166) by MTT colorimetric assay [34]. anti-HIV-1 activity (HIV-1_{IIIB} strain) of all compounds were determined by the cytopathic effect (CPE) method, which measured the viability of HIV-1_{IIIB} infected C8166 cells [36,37]. In this study, marketed drug zidovudine was used as positive control, details of experimental work and procedures followed for cytotoxicity and anti-HIV-1 assay studies are given in the supplementary part of this manuscript (Section 3.4).

3.5. Docking studies

Docking studies of four significantly active compounds (**6a**, **6b**, **6j** and **6o**) along with reference compound rilpivirine were performed using Glide 5.9 [38] (Extra Precision) running on maestro version 9.4, in order to investigate their *in-silico* inhibitory potential against three different HIV-1 RT strains. Enzyme used for the docking study were wild HIV-1 RT (Pdb ID: 3MEE), and mutant strains involved K103N (Pdb ID: 3TAM) and K103N/Y181C (Pdb ID: 4I2Q). All three selected proteins were retrieved from RCSB Protein Data Bank in complex with their co-crystallized ligands. Protein preparation wizard of Schrödinger suite was used for the preparation of selected proteins. Proteins were pre-processed separately by deleting the substrate co-factor as well as the crystallographically observed water molecules (water without H bonds), followed by optimization of hydrogen bonds. After assigning

charge and protonation states, finally energy was minimized with root mean square deviation (RMSD) value of 0.30 Å using Optimized Potentials for Liquid Simulations-2005 (OPLS-2005) force field [39]. Finally, energy minimized proteins and co-crystallized ligands were employed to build energy grids using the default value of protein atom scaling (1.0 Å) within a cubic box of dimensions centered on the centroid of the X-ray ligands pose. The structure of **6a**, **6b**, **6j**, **6o** and rilpivirine were drawn using ChemSketch and converted to 3D with the help of 3D optimization tool. By using LigPrep 2.6 module [40], the drawn ligands were geometry optimized; partial atomic charges were computed using OPLS-2005 force field. Finally, 32 poses were included with different tautomeric and steric features for docking studies. RMSD values were calculated between the experimental binding mode of co-crystallized ligands and their redocked poses in their respective proteins to ensure accuracy and reliability of the docking procedure. Finally, prepared ligands were docked with prepared proteins using Glide 5.9 module, in extra precision mode (XP). The best docked poses of ligands (with lowest Glide score value) were further analyzed and *in-silico* RT inhibitory activity of tested ligands against their respective proteins was expressed in terms their G score.

3.6. Antimicrobial activity

3.6.1. Antibacterial activity

All the synthesized compounds were evaluated for *in-vitro* antibacterial activity against two G(-)ve bacterial strains; *E. coli* (MTCC 1652) and *P. putida* (MTCC 102) and two G(+ve) bacterial strains; *S. aureus* (ATCC 25923) and *B. cereus* (MTCC 2445). Antibacterial activity of the test compounds was expressed in terms of Zone of inhibition (ZOI) and Minimum inhibitory concentration (MIC). For the experimental work, autoclaved Muller-Hilton (Himedia, India) agar medium was poured into autoclaved petri plates, further, the agar plates were swabbed with 100 µl inocula of each test organism (10⁶ CFU/ml) under aseptic condition. After adsorption, wells of 6 mm diameter were made by the sterile metallic borer and the solution of working compound was poured into the wells. The plates were incubated at 37 °C for 24 h and ZOI was calculated [41]. DMSO was used as negative control and chloramphenicol was used as reference positive control. MIC values were evaluated for all compounds using broth double dilution method. In this method, a set of tubes containing Muller Hilton broth medium with different concentrations of test compound were prepared. The tubes were inoculated with 100 µl bacterial cultures (10⁶ CFU/ml) and incubated on a rotary shaker (180 rpm) at 37 °C for 24 h under dark conditions. MIC values were defined as lowest concentration of compound that prevented the visible growth of bacteria after the incubation period [42].

3.6.2. Antifungal activity

All the synthesized compounds were also screened for *in-vitro* antifungal activity against two fungal strains *C. albicans* (MTCC 3958) and *A. niger* (MTCC 9933). Antifungal activity of the test compounds was expressed in terms of ZOI (Zone of inhibition) and MIC (Minimum inhibitory concentration). Fluconazole was used as reference drug and DMSO was used as negative control during the study. Procedure followed is described briefly; autoclaved suitable growth medium (Malt Yeast Agar for *C. albicans* and Czapek Yeast Extract Agar-CYA for *A. niger*) in double strength was poured into autoclaved petri plates. Further, the agar plates were swabbed with 100 µl inocula of each test organisms under aseptic condition. After adsorption, wells of 6 mm diameter were made by the sterile metallic borer and the solution of working compound was poured into the wells. The plates were incubated at 28 °C for 48 h and ZOI was calculated. Similarly, MIC values were

calculated using broth double dilution method for each compound, taking 100 µl inocula of each fungal culture, after incubation at 28 °C for 48 h [43,44].

4. Conclusion

In conclusion, fifteen novel 3-(6-methoxy-3,4-dihydroquinolin-1(2*H*)-yl)-1-(piperazin-1-yl)propan-1-one derivatives (**6a-o**) were designed as inhibitor of HIV-1 RT using ligand based drug design approach. Designed compounds possessed drug likeness behavior based upon the *in-silico* predicted molecular descriptors. Further, compounds were synthesized using suitable synthetic route, purified, characterized and *in-vitro* evaluated for RT inhibitory activity against wild HIV-1 RT strain. Four compounds (**6a**, **6b**, **6j** and **6o**) among the tested compounds exhibited significant inhibition of HIV-1 RT with IC₅₀ values of 9.20, 4.91, 7.68 and 6.47 µg/ml respectively. SAR studies of compounds **6a-o** revealed that, electron withdrawing group of moderate size like chloro at *meta* and electron donating group methyl at *ortho* position of phenyl ring favoured the RT inhibitory potency. Two compounds (**6b** and **6l**) exhibited significant anti-HIV activity (EC₅₀ values 4.72 and 5.45 µg/ml respectively) with safety index 24.2 and >36.7 respectively. In this study, compound **6b** exhibited significant activity against the wild HIV-1 RT as well as against HIV mediated syncytia formation.

Docking study of compounds **6a**, **6b**, **6j** and **6o** revealed that, compounds displayed good to moderate affinity against the wild RT strain (3MEE) when compared to the reference drug rilpivirine, but against the two mutant strains (3TAM and 4I2Q) these compound exhibited moderate to weak affinity. In the current study, although, none of the compounds exhibited promising HIV-1 RT inhibitory activity comparable to the reference drug efavirenz but overall studies can be helpful for further lead optimization or designing of novel potent anti-HIV agents. Antibacterial evaluation of synthesized compounds against four bacterial strains revealed that, three compounds (**6d**, **6f** and **6l**) exhibited significant growth inhibition of G(-)ve bacteria *E. coli* as well as G(+ve) *B. cereus*, while one compound **6n** significantly inhibited the growth of all tested bacterial strains. Further, three compounds (**6f**, **6l** and **6n**) significantly inhibited the growth of both the tested fungal strains.

Acknowledgments

Authors gratefully acknowledge BITS-Pilani for providing the necessary facilities to do this work. This work was carried out under a grant from Science and Engineering Research Board of Department of Science and Technology (Ref. No: SR/FT/LS-58/2011), New Delhi, INDIA. The STS program of CAS (KFJ-EW-ST-026) and Collaborative Innovation Center for Natural Products and Biological Drugs of Yunnan.

Appendix A. Supplementary material

Supplementary data associated with this article can be found, in the online version, at <http://dx.doi.org/10.1016/j.bioorg.2016.05.009>. These data include MOL files and InChIKeys of the most important compounds described in this article.

References

- [1] N.R. Faria, A. Rambaut, M.A. Suchard, G. Baele, T. Bedford, M.J. Ward, A.J. Tatem, J.D. Sousa, N. Arinaminpathy, J. Pepin, D. Posada, M. Peeters, O.G. Pybus, P. Lemey, *Science* 346 (2014) 56–61.
- [2] P. Piot, T.C. Quinn, *N. Engl. J. Med.* 368 (2013) 2210–2218.
- [3] Global HIV and AIDS statistics, <http://www.avert.org/professionals/hiv-around-world/global-statistics#footnote2_gtuftce7> (accessed on 4 November 2015).

- [4] 2014 Global Statistics, <<http://www.unaids.org/en/resources/campaigns/HowAIDSchangedeverything/>> factsheet (accessed on 8 November 2015).
- [5] P. Zhan, C. Pannecouque, E. De Clercq, X. Liu, *J. Med. Chem.* (2015), <http://dx.doi.org/10.1021/acs.jmedchem.5b00497> (in press).
- [6] P. Chong, P. Sebahar, M. Youngman, D. Garrido, H. Zhang, E.L. Stewart, R.T. Nolte, L. Wang, R.G. Ferris, M. Edelstein, K. Weaver, A. Mathis, A. Peat, *J. Med. Chem.* 55 (2012) 10601–10609.
- [7] H. Kim, H. Gim, M. Yang, J.H. Ryu, R. Jeon, *Heterocycles* 71 (2007) 2131–2154.
- [8] M. Yu, E. Fan, J. Wu, X. Liu, *Curr. Med. Chem.* 18 (2011) 2376–2385.
- [9] N. Sluis-Cremer, M.A. Wainberg, R.F. Schinazi, *Future Microbiol.* 10 (2015) 1773–1782.
- [10] E.L. Asahchop, M.A. Wainberg, M. Oliveira, H. Xu, B.G. Brenner, D. Moisi, I.R. Ibanescu, C. Tremblay, *AIDS (London, England)* 27 (2013) 879–887.
- [11] K. Das, J.D. Bauman, A.D. Clark, Y.V. Frenkel, P.J. Lewi, A.J. Shatkin, S.H. Hughes, E. Arnold, *Proc. Natl. Acad. Sci. USA* 105 (2008) 1466–1471.
- [12] A. Mitchinson, A. Nadin, *J. Chem. Soc. Perkin Trans. 1* (18) (1999) 2553–2582.
- [13] J.P. Michael, *Nat. Prod. Rep.* 25 (2008) 166–187.
- [14] S. Kumar, S. Bawa, H. Gupta, *Mini. Rev. Med. Chem.* 9 (2009) 1648–1654.
- [15] V. Sridharan, P.A. Suryavanshi, J.C. Menendez, *Chem. Rev.* 111 (2011) 7157–7259.
- [16] G.A. Jacoby, M.A. Corcoran, D.C. Hooper, *Antimicrob. Agents Chemother.* 59 (2015) 6689–6695.
- [17] S.B. Wang, X.F. Wang, B. Qin, E. Ohkoshi, K.Y. Hsieh, E. Hamel, M.T. Cui, D.Q. Zhu, M. Goto, S.L. Morris-Natschke, K.H. Lee, L. Xie, *Bioorg. Med. Chem.* 23 (2015) 5740–5747.
- [18] D.S. Su, J.J. Lim, E. Tinney, B.L. Wan, M.B. Young, K.D. Anderson, *Bioorg. Med. Chem. Lett.* 19 (2009) 119–123.
- [19] J. Zhang, P. Zhan, J. Wu, Z. Li, Y. Jjiang, W. Ge, C. Pannecouque, E. De Clercq, X. Liu, *Bioorg. Med. Chem.* 19 (2011) 4366–4376.
- [20] Z. Liu, W. Chen, P. Zhan, E. De Clercq, C. Pannecouque, X. Liu, *Eur. J. Med. Chem.* 87 (2014) 52–62.
- [21] Qik-prop, New York, Schrödinger, LLC, Version 3.7, 2013.
- [22] F. Cheng, W. Li, Y. Zhou, J. Shen, Z. Wu, G. Liu, *J. Chem. Inf. Model* 52 (2012) 3099–3105.
- [23] D. Lagorce, O. Sperandio, J.B. Baell, M.A. Miteva, B.O. Villoutreix, *Nucl. Acids Res.* 43 (2015) W200–W207.
- [24] M. Ghate, S. Deshpande, S. Tripathy, M. Nene, P. Gedam, S. Godbole, M. Thakar, A. Risbud, R. Bollinger, S. Mehendale, *Int. J. Infect. Dis.* 13 (2009) e1–e8.
- [25] S.D. Patel, D.M. Kinariwala, T.B. Javadekar, *Indian J. Sexual Transm. Dis.* 32 (2011) 90–93.
- [26] E. Ramesh, R.D. Manian, R. Raghunathan, S. Sainath, M. Raghunathan, *Bioorg. Med. Chem.* 17 (2009) 660–666.
- [27] L.J. Lombardo, A. Camuso, J. Clark, K. Fager, J. Gullo-Brown, J.T. Hunt, *Bioorg. Med. Chem. Lett.* 15 (2005) 1895–1899.
- [28] R.L. Jarvest, S.A. Armstrong, J.M. Berge, P. Brown, J.S. Elder, M.J. Brown, *Bioorg. Med. Chem. Lett.* 14 (2004) 3937–3941.
- [29] J.M. Urbina, J.C. Cortes, A. Palma, S.N. Lopez, S.A. Zacchino, R.D. Enriz, *Bioorg. Med. Chem.* 8 (2000) 691–698.
- [30] P. Bendale, S. Olepu, P.K. Suryadevara, V. Bulbule, K. Rivas, L. Nallan, *J. Med. Chem.* 50 (2007) 4585–4605.
- [31] M. Gutierrez, U. Carmona, G. Vallejos, L. Astudillo, *Z. Naturforsch. C* 67 (2012) 551–556.
- [32] Qikprop, User Manual, Schrödinger, LLC, Version 3.8, 2013, pp. 2–5 (Chapter 1).
- [33] K.K. Roy, S. Tota, T. Tripathi, S. Chander, C. Nath, A.K. Saxena, *Bioorg. Med. Chem.* 20 (2012) 6313–6320.
- [34] P. Ashok, S. Chander, J. Balzarini, C. Pannecouque, S. Murugesan, *Bioorg. Med. Chem. Lett.* 25 (2015) 1232–1235.
- [35] J. Eberle, C.W. Knopf, *Methods Enzymol.* 275 (1996) 257–276.
- [36] G.H. Zhang, Q. Wang, J.J. Chen, X.M. Zhang, S.C. Tam, Y.T. Zheng, *Biochem. Biophys. Res. Commun.* 334 (2005) 812–816.
- [37] R.R. Wang, Q. Gu, Y.H. Wang, X.M. Zhang, L.M. Yang, J. Zhou, J.J. Chen, Y.T. Zheng, *J. Ethnopharmacol.* 117 (2008) 249–256.
- [38] Glide, Schrödinger, LLC, New York, version 5.9, 2013.
- [39] W.L. Jorgensen, D.S. Maxwell, R.J. Tirado, *J. Am. Chem. Soc.* 118 (1996) 11225–11236.
- [40] Lig-Prep, Schrödinger, LLC, New York, version 2.6, 2013.
- [41] P.A. Wayne, *Clinical and Laboratory Standards Institute*, 7th edition, 2006, pp. M7–A7.
- [42] J.M. Andrews, *J. Antimicrob. Chemother.* 48 (2001) 5–16.
- [43] S. Magaldi, S. Mata-Essayag, C. Hartung de Capriles, C. Perez, M.T. Colella, C. Olaizola, Y. Ontiveros, *Int. J. Infect. Dis.* 8 (2004) 39–45.
- [44] S. Chander, P. Ashok, Y.T. Zheng, P. Wang, K.S. Raja, A. Taneja, S. Murugesan, *Bioorg. Chem.* 64 (2016) 66–73.